[UCI]I804:24011-200000235892

2008년 2월
박사학위논문

Molecular mechanisms of senescence-dependent mismatch repair dysfunction

조선대학교 대학원

의학과

조 향 훈

Molecular mechanisms of senescence-dependent mismatch repair dysfunction

노화과정에서 발생하는 mismatch 복구기능 저하 기전

2008 년 2 월 25 일

조선대학교 대학원

의학과

조 향 훈

Molecular mechanisms of senescence-dependent mismatch repair dysfunction

지도교수 유 호 진

이 논문을 의학박사학위신청 논문으로 제출함.

2007 년 10 월 일

조선대학교 대학원

의학과

조 향 훈

조 향 훈의 박사학위 논문을 인준함

위원장	조선 대학교	교수	장인엽	인
위 원	조선 대학교	교수	전제열	인
위 원	서남 대학교	교수	윤상필	인
위 원	조선 대학교	교수	황 걸	인
위 원	조선 대학교	교수	유호진	인

2007 년 12 월

조선대학교 대학원

CONTENTS

LIST OF FIGURE

Molecular mechanisms of senescence-dependent mismatch repair dysfunction

Cho Hyang Hoon

Advisor : Prof. Ho Jin You, Ph.D., M.D.

Graduate School of Chosun University

Medical School

ABSTRACT

DNA damage and mutations in the genome increase with age. To determine the potential mechanisms of senescence-dependent increases in genomic instability, we analyzed DNA mismatch repair (MMR) efficiency in young and senescent human colonic fibroblast and human embryonic lung fibroblast. It was found that MMR activity is significantly reduced in senescent cells. Western blot and immunohistochemistry analysis revealed that hMSH2 and MSH6 protein (MutSα complex), which is a known key component in the MMR pathway, is markedly down-regulated in senescent cells. Moreover, the addition of purified MutSα to

extracts from senescent cells led to the restoration of MMR activity. Semiquantitative RT-PCR analysis exhibited that MSH2 mRNA level is reduced in senescent cells. In addition, a decrease in E2F transcriptional activity in senescent cells was found to be crucial for MSH2 suppression. E2F1 siRNA expression reduced hMSH2 expression and MMR activity in young human primary fibroblast cells. Importantly, expression of E2F1 in quiescent cells restored the MSH2 expression as well as MMR activity, whereas E2F1 infected senescent cells exhibited no restoration of MSH2 expression and MMR activity. These results indicate that the suppression of E2F1 transcriptional activity in senescent cells lead to stable repression of MSH2, followed by a induction of MutSα dysfunction, which results in a reduced cellular MMR capacity in senescent cells.

I. INTRODUCTION

Aging is a multifactorial phenomenon characterized by a time dependent decline in the functional reserve of most organ systems. Although several theories have been proposed to explain this process, the underlying mechanisms of aging have not been elucidated. The somatic mutation theory of aging proposes the age-related accumulation of DNA damage, as a fundamental mechanism underlying aging, and this theory is supported by observations that DNA damage and mutations in the genome increase with age (1, 2). Because DNA repair is tightly linked with levels of DNA damage and mutagenesis, several studies have focused on the potential role of DNA repair in aging. In general, these studies have revealed that the ability of cells to repair DNA declines with age (3-8). A reduced ability to repair DNA damage is also important in carcinogenesis, as mutations are known to be early events in cancer development (1, 2, 9-11). Accordingly, most human cancers develop after 50-60 years of age (10), and perhaps the decline in DNA repair with age explains increased cancer incidence in the elderly. However, the contributing mechanisms responsible for this age-dependent decline in DNA repair activity need to be elucidated.

DNA mismatch repair (MMR) is an important cellular pathway that facilitates genome stability by excising mismatched DNA nucleotides (12, 13). In humans, a defective MMR system results in a high cancer predisposition, as shown by hereditary non-polyposis colon cancer (HNPCC), in which the majority of affected

individuals have inherited defective copies of the essential MMR genes *MSH2*, *hMLH1* or *MSH6* (14-16). Loss of MMR activity leads to increased mutation rates, associated microsatellite instability (MSI), and the accumulation of mutations that play a role in carcinogenesis and are characterized by a mutator phenotype (12, 13). Aged cells showed significantly higher rates of MSI (17-20), which is likely to be responsible for a predisposition to cancer in the elderly, particularly in view of the role of genetic instability in carcinogenesis. Therefore, the MMR system may show reduced functionality with age. However, there is no direct evidence of the effect of age on MMR activity or on the regulation of specific MMR gene expressions.

In this study, we examined the MMR system in human colonic fibroblast (CCD-18Co) and human embryonic lung fibroblast (IMR90) with respect to senescence. Our results show that MSH2 and MSH6 expression is markedly suppressed in senescent cells, resulting in a reduced cellular capacity to repair mismatches. In addition, we demonstrate that the senescence-related down-regulation of E2F transcriptional activity contributes to the stable suppression of MSH2 expression.

II. MATERIALS AND METHODS

Cell culture. The CCD-18Co and IMR90 (American Type Culture Collection) were maintained in Earle's minimum essential medium (EMEM) supplemented with 10 % fetal bovine serum (FBS). The HEC59 (a gift from Dr. Richard Boland**, Baylor College of Medicine in Dallas, Texas**) were cultured in Iscove's modified Dulbeco's medium (IMDM) supplemented with 10 % FBS.

Animals and tissue preparation. The senescence accelerated mouse (SAM) has been established as a murine model of accelerated aging by Toshio Takeda (21). SAMP (prone) strains are unique and appropriate models for studies on aging because the strains have an "accelerated senescence" phenotype. SAMP strains include SAMP1, SAMP2, SAMP3, SAMP6, SAMP7, SAMP8, SAMP9, SAMP10 and SAMP11. Symptoms of accelerated senescence, such as a hair loss, skin coarseness, cataract, increased lordokyphosis and systemic senile amyloidosis, are a common characteristic in SAM strains. Otherwise, SAMR strains, including SAMR1, SAMR4 and SAMR5, are senescence-resistant inbred strains. SAMP strains show markedly shorter average life span compared to SAMR. The SAMP1 mice exhibited increased chromosome aberration (22), mutation of *hprt* genes (22) and the strong correlation of DNA damage and aging process (23). Therefore, we used SAMP1 and SAMR1 for our experiments. SAMP1 and SAMR1 strains were 4-, 32-weeks-old at the time of the experiments. These mice were kindly provided

by Toshio Takeda (Kyoto University, Kyoto, Japan). All animals were individually housed in standard Plexiglas laboratory cages (550×350×260 mm) within a large well-ventilated room with a constant temperature of 23 °C with a 12-hour light/dark cycle, and free access to food and water.

SAM was anesthetized by pentobarbital (15 mg/kg: intraperitoneal injection) and perfused transcardially with 500 ml 0.02 M phosphate-buffered saline (PBS; pH 7.4) followed by 500 ml 4 % paraformaldehyde in 0.1 M phosphate buffer (pH 7.4). The large intestine was dissected out and further fixed with the same fixative overnight. Then the tissues were soaked in 30 % sucrose in PBS and frozen. They were serially sectioned at a thickness of 10 μm and then from mounted on 3-aminopropyl-tri-ethoxylsilane-coated glass slides.

Immunohistochemistry. The section were treated with methanol containing 0.3 % H_2O_2 for 20 min at room temperature and washed with PBS. They were incubated overnight with rabbit polyclonal antisera against MSH2, MSH6 and OGG1 (1:100; Santa Cruz Biotech, CA, USA), and treated with biotinylated goat antibody against rabbit IgG (1:200; Vector Laboratories, CA). After washing, the sections were incubated in peroxidase-conjugated avidin-biotin-peroxidase complex (1:100; ABC kit, Vector Laboratories) and then dehydrated in ethyl alcohol, cleared with xylene and sealed with coverslips.

Western blotting. Western blot analysis was performed as describe previously

(24) using the following antibodies: MSH2, MSH6, MSH3, MLH1, PMS2, E2F1, OGG1 and α-tubulin (Santa Cruz Biotech). The mucosa of the large intestine from SAM was scraped from underlying muscular layers and homogenized in buffer containing 50 mM Hepes, PH 7.5, 150 mM NaCl, 100 mM NaF, 10 mM EDTA, 10 mM $Na_4P_2O_7$, 1 % Nonidet P-40, 1 mM phenylmethylsulfonyl fluoride (PMSF), 10 μg/ml leupeptin, 10 μ/ml aprotinin, 1 mM Na_3VO_4, and 5 mM NaF). 20 μg protein per lane was electrophoresed on the 10 % SDS polyacrylamide gels. The proteins were blotted onto the Hybon ECL membranes (Amersham-Pharmacia, Biotech) and the blotted proteins were detected using an enhanced chemiluminescence detect system (iNtRON, Biotech, Seoul, Korea).

Senescence-associated β-galactosidase staining. The assay of senescence-associated β-galactosidase activity was carried out according to the procedure as described (25). Briefly, cells were washed in PBS, fixed with 2 % formaldehyde, 0.2 % glutaraldehyde in PBS for 5 min at room temperature. Cells were then washed with PBS twice and incubated at 37 °C (no CO_2) with freshly prepared senescence-associated β-galactosidase (SA β-gal) staining solution (1 mg/ml X-Gal; 40 mM citric acid/sodium phosphate buffer pH 6.0; 5 mM potassium ferrocyanide; 5 mM potassium ferricyanide; 150 mM sodium chloride; 2 mM magnesium chloride). Dishes were incubated at 37 °C (CO_2 free incubator) overnight and then analyzed immediately for positive staining.

Semiquantitative RT-PCR. Semiquantative RT-PCR analysis was perforemd as described previsouly (24). The primers used for the PCR are as follows: *MSH2* forward, 5'-GTCGGCTTCGTGCGCTTCTTT-3'; *MSH2* reverse, 5'-TCTCTGGCC ATCAACTGCGGA-3'; *MSH6* forward, 5'-CCTTCAGCCACCAAACAAGCA-3'; *MSH6* reverse, 5'-CTGCCACCACTTCCTCATCCC-3'; *MSH3* forward, 5'-ACAGCCATGCTTTCCAGGCA-3'; *MSH3* reverse, 5'-ATACAGCATCAAGCCGG GCA-3' ; *MLH1* forward, 5'-GCAAGCTCCTGGGCTCCAAT-3'; *MLH1* reverse, 5'-CTTCAGCAGGGGCTGGGAGT-3' and *GAPDH* forward, 5'-CCATGGAGAAGG CGGGG-3'; GAPDH reverse, 5'- CAA AGT TGTCATGGATGACC-3'.

Purification of human MutSα. Human MutSα was purified from the nuclear extracts of HeLaS3 cells, as described with some modifications (24, 26).

DNA constructs. The E2F reporter construct was kindly provided by Dr. Walter Heyns (Catholic University of Leuven, Leuven, Belgium). The p1116, p99 and m-p66 MSH2 promoter-reporter constructs were described previously (24). The m-p1116 mutant construct, which included four mutated E2F binding site, was made by a PCR from the p1116 construct using the primers (5'-GGAGGCGGATATCAGCTTAGTGGG-3', 5'-AGCGTGCGATAGAAGCTGGGC-3', 5'-GGTTTCATAGCGACCTAGGCG-3',

5'-CTGGCGTATTACGTTTGTCT-3`). The underlined letter indicates the nucleotide substitutions of the insert mutations. E2F1 siRNA and LacZ siRNA were prepared as described previously (24). Human *E2F1* cDNA, was amplified by RT-PCR using the *E2F1* oligo primer (5'-TCT AGA ATG CCG AAG CGT GGG AAA AAG G-3', 5'-GGT ACC TCA CAG TGC TAG GTA TAG GGT G-3') from human fibroblast GM00637 cells.

Construction of adenoviral vector encoding E2F1 cDNA. The *E2F1* cDNA was inserted into Adeno-X viral DNA of Adeno-X Expression System (Clontech Co., Palo Alto, CA, USA). For virus collection, the transfected HEK293 cells were lysed with three consecutive freeze-thaw cycles, and the virus was collected from the supernatant. The virus titer was approximately $1x10^7$ pfu/ml, which was determined using an end-point dilution assay. A vector carrying the β-galactosidase gene *LacZ* (Ad-LacZ) was used to monitor efficiency of transduction by the viral vectors and nonspecific transgene expression controls.

Promoter Luciferase activity assays. The reporter plasmids were transiently transfected into the cells using the lipofectamine (Life Technologies, Inc), and promoter luciferase activity was determined as described previously (27).

Chromatin Immunoprecipitation Assays. Chromatin Immunoprecipitation was performed as described (24).

In vitro MMR assay. The *in vitro* MMR activities of the young and senescent cells were measured using the M13mp2 lacZ α-complementation method as described previously (24, 28). Briefly, the MMR repair activities were investigated by using heteroduplex DNA that contained a G-T, G-G or A-C mismatch or a single loop with two extrahelical nucleotides in the *lacZ* α-complementation gene in the M13mp2 DNA. Substrates used are a base-base mismatch at position 87 for A-C, 88 for G-T and G-G, and a two base loop at position 90 of the *lacZ* α-complementation gene. The nick is only (-) strand of M13mp2 substrates. The repair reactions contained 30 mM Hepes (pH 7.8), 7 mM $MgCl_2$, 4 mM ATP, 200 μM each of CTP, GTP and UTP, 100 μM each of dATP, dGTP, dTTP and dCTP, 40 mM creatine phosphate, 100mg/ml creatine phosphokinase, 15 mM sodium phosphate, 5 ng of purified heteroduplex DNA and 50 μg of the extracted nuclear protein. The incubation was carried out at 37 °C for 30 min. In the complementation studies, the repair assays were carried out as described above, except that the extracts (50 μg) were supplemented with 0.1 μg of hMutSα. The DNA heteroduplex was then purified and introduced into a *mutS* strain via electroporation. When introduced into an *E. coli* strain deficient in methyl-directed heteroduplex repair (*mutS*), an unrepaired mismatch heteroduplex yields a "mixed" plaque phenotype due to expression of both strands of the M13mp2 DNA. However, if repair of the mismatched base situated on the (–) strand takes place during incubation with a human cell extract, the percentage of mixed plaques decreases

and the percentage of colorless (+) plaques increases, such that ratio of pure blue to pure colorless plaques is reduced. The DNA mismatch repair activity was calculated from the following formula: 100 % x [1 − (percentage of mixed colored plaques developed from the reaction containing the extract/ percentage of mixed colored plaques developed from the reaction containing no extract)]. We also used substrates containing A-T at position 87 and G-C at position 88 as a control. Using these substrates, we confirmed that substrates containing A-T at position 87 and G-C at position 88 exhibited 100 % white colony and blue colony, respectively.

III. RESULTS

Constitutive level of MSH2 and MSH6 protein reduces with senescence

We examined MMR protein expression during the replicative senescence of CCD-18Co human colonic fibroblasts and IMR90 human embryonic lung fibroblasts. To eliminate possible variations due to culture conditions, all growth conditions used for primary fibroblast cells were identical. CCD-18Co and IMR90 cells were grown under the standard 3T3 protocol ($3x10^5$ cells transferred to a new dish every 3 days). The CCD-18Co and IMR90 cells became senescent at population doubling levels (PDLs) of 45 and 57, respectively, where approximately 80 % cells were shown to be positive for SA-β-gal, a histochemical marker of replicative senescence (Figure 1A, C, D). Young, intermediate and senescent CCD-18Co cells used in this experiment were at PDLs of 24, 38 and 45, respectively, and the young, intermediate and senescent IMR90 cells used in this experiment were at PDLs of 23, 42 and 57, respectively.

To investigate the levels of mismatch repair proteins, such as MSH2, MSH6, MSH3, MHL1, and PMS2, in young, intermediate and senescent CCD-18Co and IMR90 cells, we used SDS-polyacrylamide-gel electrophoresis (SDS-PAGE) to separate whole cell extracts of protein form young and senescent cells. Western blotting with a specific polyclonal antibody against MSH2, MSH6, MSH3, MHL1, and PMS2 showed a significantly decrease in the level of MSH2 and MSH6 protein,

correlating with the passage number increased. However, the other MMR gene expression levels were unaffected by the increase in passage number (Figure 1B). MSH2and MSH6 signal intensities were calculated as percentages ± s.d. of the α-tubulin signal. The levels of MSH2 protein expression were reduced by 85 ± 3.1 or 87 ± 3.4 % in senescent CCD-18Co and IMR90 cells, respectively, compared to the early passage cells, and the levels of MSH6 protein expression were reduced by 77 ± 2.8 or 79 ± 3.3 % in senescent CCD-18Co and IMR90 cells, respectively, compared to the early passage cells (Figure 1C). These results demonstrate that MSH2 and MSH6 are down-regulated in senescent cells.

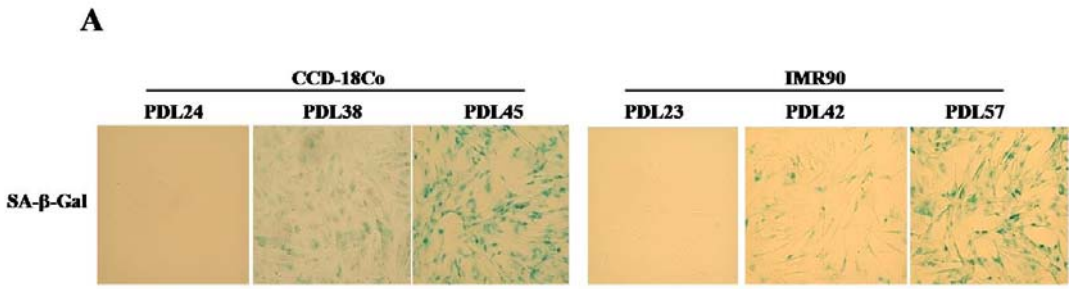
A
CCD-18Co
IMR90
PDL24
PDL38
PDL45
PDL23
PDL42
PDL57
SA-β-Gal

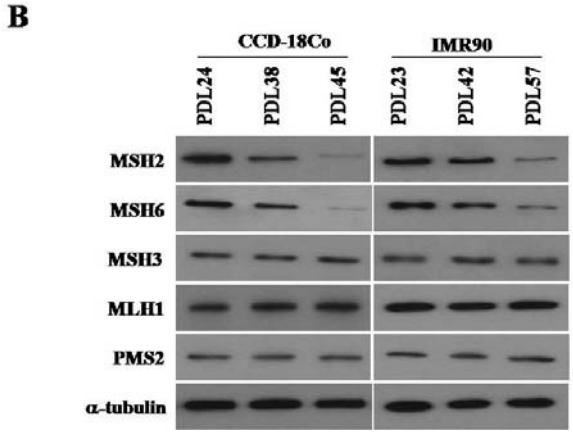
B
CCD-18Co
IMR90
PDL24
PDL38
PDL45
PDL23
PDL42
PDL57
MSH2
MSH6
MSH3
MLH1
PMS2
α-tubulin

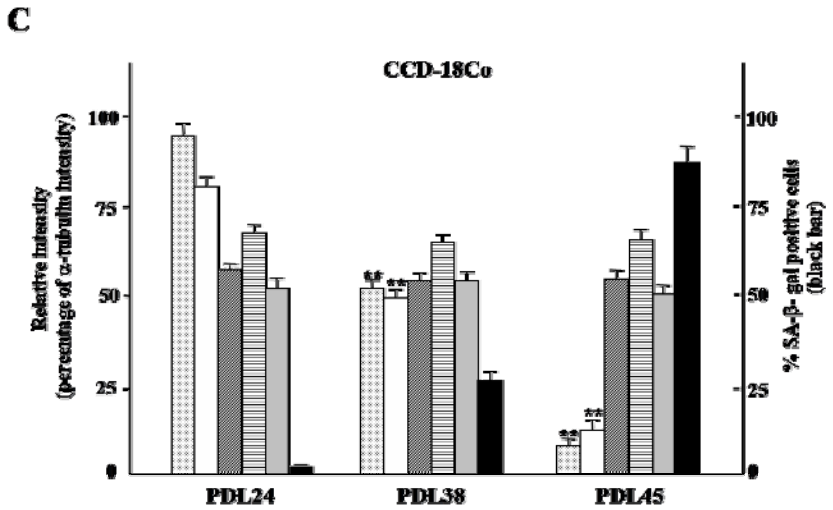
C
CCD-18Co
Relative intensity
(percentage of α-tubulin intensity)
% SA-β- gal positive cells
(black bar)
100
75
50
25
0
PDL24
PDL38
PDL45

D

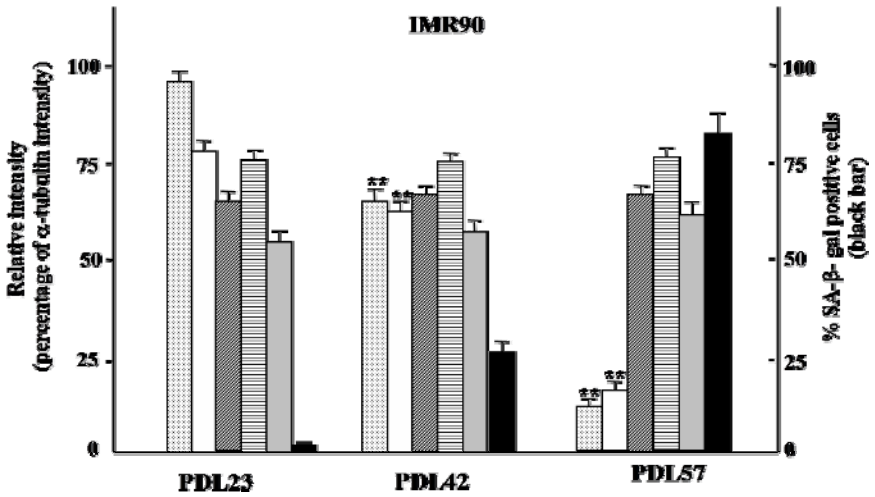
IMR90
Relative intensity
(percentage of α-tubulin intensity)
% SA-β- gal positive cells
(black bar)
100
75
50
25
0
PDL23
PDL42
PDL57

Figure 1 Expression of mismatch repair protein levels in young and senescent cells. (A) Senescence associated β-galactosidase (SA-β-gal) staining in young and senescent CCD-18Co and IMR90 cells. CCD-18Co cells were used at population doubling levels (PDLs) of 24, 38 and 45, respectively, and IMR90 cells were used at population doubling levels (PDLs) of 23, 42 and 57, respectively. (B) Protein extracts of CCD-18Co and IMR90 cells were examined by Western blotting using anti-MSH2, anti-MSH6, anti-MSH3, anti-MLH1 and anti-PMS2 antibodies. α-tubulin was used as a loading control. (C-D) The quantified levels of MSH2, MSH6, MSH3, MLH1 and PMS2, relative to those of α-tubulin. Dotted bars, MSH2; white bars, MSH6; hatched bars, MSH3; striped bars, MLH1; shaded bars, PMS2; black bars, fraction of SA-β-gal-positive CCD-18Co (C) and IMR90 (D) cells. Values are means ±s.d. of three separate experiments. ** denotes $P<0.01$.

MSH2 and MSH6 are lower in the large intestine of senescence accelerated mouse

To investigate the age-related changes in MSH2 and MSH6 protein expression in the large intestine of the senescence accelerated mouse (SAM), western blot analysis of MSH2 and MSH6 expression were performed. The SAM strain was established as a novel murine model of senescence acceleration and age-associated disorders (29).

The strains that are prone to signs of accelerated senescence are referred to as senescence-accelerated mouse prone (SAMP) and strains resistant to early aging are termed senescence-accelerated mouse resistant (SAMR) (30). SAMP mice have a mean life expectancy of 12-15 months. They develop normally until the age of 4 months and then reveal signs of accelerated aging (30). Western blot analysis showed that the MSH2 and MSH6 protein levels of the large intestine were markedly reduced in the 32-week SAMP strain only (Figure 2A). Immunohistochemistry staining using same antibody also confirmed that the expression levels of MSH2 and MSH6 were significantly reduced in the large intestine of 32-week SAMP strain (Figure 2B). We also checked the expression level of 8-oxoguanine-DNA glycosylase (Ogg1), which is a bifunctional enzyme with both 8-oxoG excision activity and weak AP lyase activity, in the same samples, and found that he expression levels of Ogg1 were not reduced in the large intestine of 32-week SAMP strain.

A

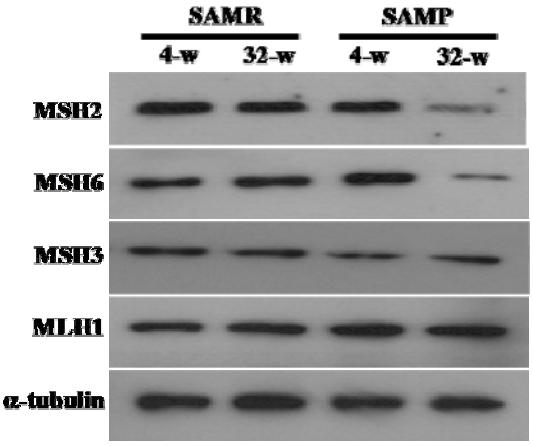
SAMR
SAMP
4-w
32-w
4-w
32-w
MSH2
MSH6
MSH3
MLH1
α-tubulin

B

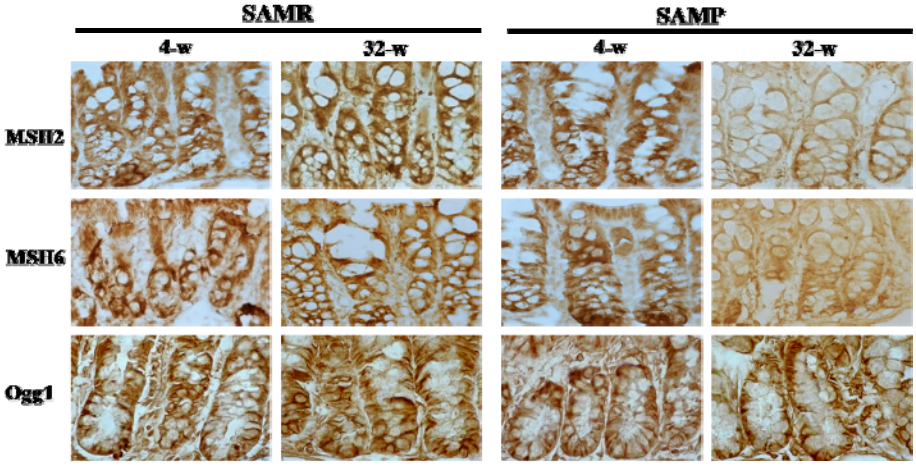
SAMR
SAMP
4-w
32-w
4-w
32-w
MSH2
MSH6
Ogg1

Figure 2 Age-dependent changes in MSH2 and MSH6 protein. (A) Protein extracts of 4- and 32-week (w) old senescence accelerated mouse resistant (SAMR) and senescence accelerated mouse prone (SAMP) large intestine were examined by Western blotting using anti-MSH2, anti-MSH6, ant-MSH3, anti-MLH1 antibodies. α-tubulin was used as a loading control. (B) MSH2, MSH6 and Ogg1 protein expression of large intestine in SAMP and SAMR was confirmed by immunohistochemistry.

Mismatch repair activity is attenuated in senescent CCD-18Co and IMR90 cells

To compare the mismatch repair activity in young and senescent CCD-18Co and IMR90 cells, different cell extracts were tested for their ability to repair A:C, G:G and G:T mispairs and a loop with two extrahelical bases. Unrepaired heteroduplex plasmids generated mixed-color colonies when transfected into *E. coli*. Repaired reaction by cell lysates resulted in decreased numbers of mixed color colonies. As shown in Figure 3, young cells efficiently repaired all three mispairs (Figure 3A) and insertion/deletion loop (Figure 3C). However, senescent cells were deficient in MMR function and had limited MMR activities. As MSH2 combines with MSH6 (to form the MutSα complex) and MutSα is responsible for the initial recognition of a mismatched nucleotide (31), it was decided to determine whether the addition of purified human MutSα to senescent cell extracts could restore MMR activity. Thus, extracts from senescent cells in the presence or absence of purified MutSα were tested for their ability to correct a heteroduplex containing a G:G mismatch and a loop with two extrahelical bases. We found that the addition of purified recombinant MutSα to extracts of senescent cells resulted in the restoration of G:G mismatch repair (Figure 3B) and insertion/deletion loop repair (Figure 3C). As controls, MMR activities were measured in a *MSH2*-deficient HEC59. The HEC59 extracts were deficient in the repair of G:G mismatch and insertion/deletion loop , whereas the addition of purified MutSα to the HEC59 extracts restored this repair (Figure 3B, C). These results suggest that senescent cells lack a functional MutSα, which leads to reduced MMR activity.

A

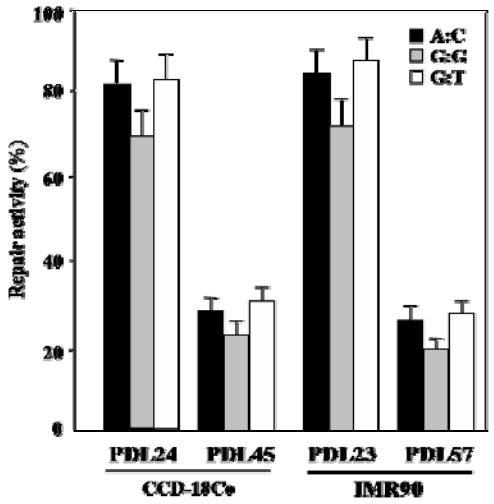
100
80
60
40
20
0
Repair activity (%)
A:C
G:G
G:T
PDL24
PDL45
PDL23
PDL57
CCD-18Co
IMR90

B

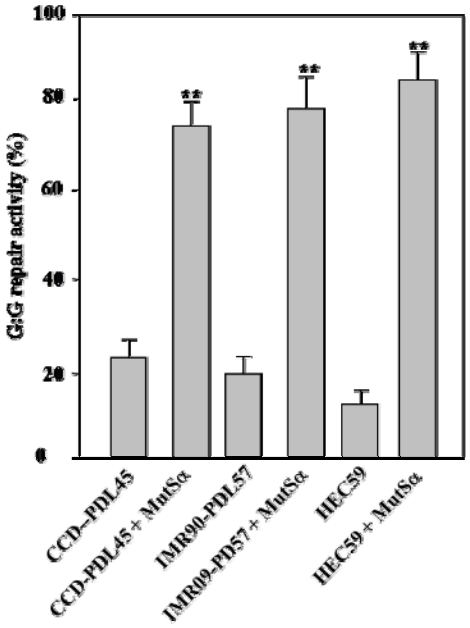
100
80
60
40
20
0
G:G repair activity (%)
**
**
**
CCD--PDL45
CCD-PDL45+ MutSα
IMR90-PDL57
IMR09-PD57+ MutSα
HEC59
HEC59+ MutSα

C

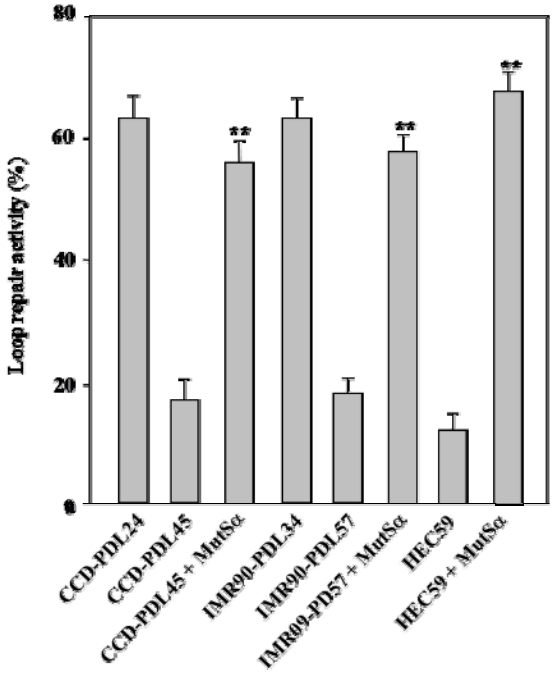
Loop repair activity (%)
80
60
40
20
0
**
**
**
CCD-PDL24
CCD-PDL45
CCD-PDL45 + MutSα
IMR90-PDL34
IMR90-PDL57
IMR09-PD57 + MutSα
HEC59
HEC59 + MutSα

Figure 3 The mismatch repair activity in young and senescent CCD-18Co and IMR90 cells. (A) The cells extracts of the young and senescent cells were compared in terms of A:C (in black), G:G (in gray) and G:T (in white) mismatch repair efficiencies. The results are based on counting 500-1,000 plaques per variable. Repair efficiency was determined by calculating the percentage reduction in mixed color colonies. Values are means ±s.d. of three separate experiments. (B) The cells extracts of senescent CCD-18Co and IMR90 cells, and of HEC59 cells were assayed for G:G mispair repair in the presence or absence of 0.1 μg of purified MutSα. The results are based on counting 500-1,000 plaques per variable. Repair efficiency was determined by calculating the percentage reduction in mixed color colonies. Values are means ±s.d. of three separate experiments. ** denotes $P<0.01$. (C) The insertion/deletion loop repair activity in young and senescent CCD-18Co and IMR90 cells. The cells extracts of young and senescent CCD-18Co and IMR90 cells, and of HEC59 were assayed for the repair efficiency of the two nucleotide insertion/deletion loop in the presence or absence of 0.1 μg of purified MutSα. The results are based on counting 500-1,000 plaques per variable. Results are average of three independent experiments, and values are means ±s.d. of three separate experiments. denotes $P<0.01$.

Reduced transcriptional activity of E2F1 in senescent cells leads to a reduction in MSH2 promoter activity

To examine whether the decreased MSH2 and MSH6 protein expression in senescent cells occurs at the transcription level, semiquantitative RT-PCR was carried out using specific primers for MSH2, MSH6, MSH3 and MLH1. The PCR exponential phase was obtained and the optimal number of PCR cycles (24 cycles, data not shown) was determined. The results showed that the MSH2 mRNA was down-regulated in senescent cells (Figure 4). The MSH2 mRNA levels were reduced by 85 ± 5.4 or 90 ± 4.3 % in senescent CCD-18Co or IMR90 cells versus the young cells, respectively. However, the MSH6, MSH3 and MLH1 mRNA level was only slightly reduced in senescent cells. It has been reported that MSH2 is essential to stabilize MSH6 (32). Therefore, a significant decrease in the MSH2 level might disrupt the stabilization of MSH6, which can explain the marginal MSH6 expression level observed in the senescent cells.

Next, the potential mechanisms responsible for the observed transcriptional inhibition of MSH2 in senescent cells were examined. Because E2F is known to be repressed in senescent human cells, and MSH2 is an E2F-responsive gene (24, 33, 34), we focused on the transcription factor E2F. To confirm the reduced transcriptional activity of E2F in senescent cells, young and senescent cells were transiently transfected with an E2F reporter construct containing six E2F responsive sites, and luciferase activity was determined 24 h after transfection. As

we expected, the senescent cells showed significantly lower levels of E2F controlled luciferase activity than the young cells (Figure 5A).

We further analyzed the relationship between reduced E2F activity and MSH2 expression, using reporter constructs encoding luciferase under the control of the MSH2 promoter. DNA sequence analysis indicated the MSH2 promoter contains several putative E2F binding sites (Figure 5B). Young and senescent cells were transfected with one of the four MSH2 promoter–luciferase constructs, namely: p99, spanning positions -1 to - 99 of the promoter, including one E2F-binding motif; m-p99, spanning positions -1 to - 99 of the promoter, including a mutated E2F-binding motif; p1116, spanning positions -1 to -1116 of the promoter, including four E2F-binding motifs; or m-p1116, spanning positions -1 to -1116 of the promoter, including four mutated E2F-binding motifs. In transient-transfection assays using young and senescent CCD-18Co and IMR90 cells, both p99 and p1116 transfections resulted in a marked luciferase activity reduction in the senescent cells (Figure 5B). However, the luciferase activities of m-p99 and m-p1116 were similar in young and senescent cells. These site-directed mutagenic studies strongly suggest that reduced E2F activity contributes to the suppression of MSH2 promoter activity in senescent cells.

In order to provide evidence for a direct interaction of E2F1 to these E2F binding sites of the MSH2 promoter *in vivo*, we performed chromatin immunoprecipitation (ChIP) assays in young and senescent cells. The young cells showed a strong signal

for an association between E2F1 and MSH2 promoter encompassing E2F1, whereas the amount of E2F1 bound to the MSH2 promoter significantly decline in the senescent cells (Figure 6). The PCR product was not immunoprecipitated when a non-specific antibody (anti-mouse IgG) was used in identical experiment, and the amount pf E2F1 bound to the β-actin promoter was not detected. These results suggest that E2F1 binding to the MSH2 promoter is reduced in senescent cells.

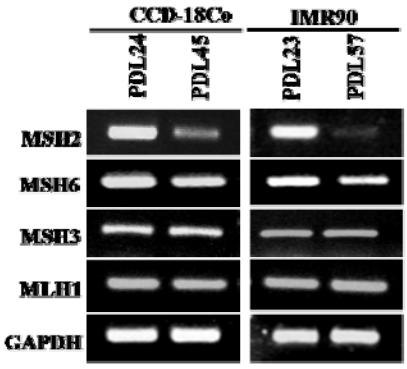
CCD-18Co
IMR90
PDL24
PDL45
PDL23
PDL57
MSH2
MSH6
MSH3
MLH1
GAPDH

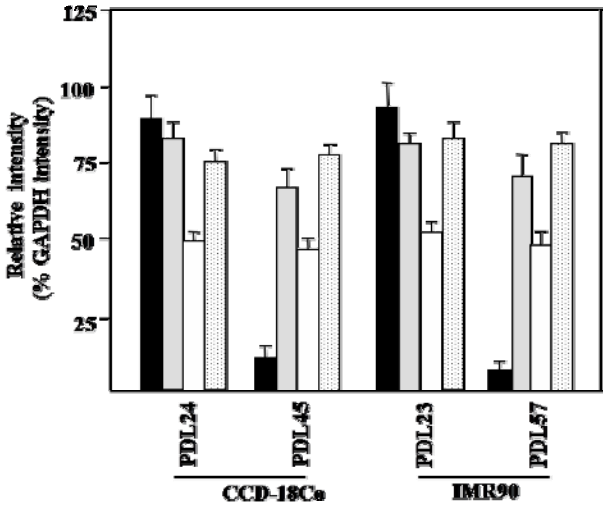
125
100
75
50
25
Relative intensity
(% GAPDH intensity)
PDL24
PDL45
PDL23
PDL57
CCD-18Co
IMR90

Figure 4 Senescence-dependent changes in MSH2 mRNA. Left panels, The mRNA expressions of MSH2, MSH6, MSH3 and MLH1 in young and senescent CCD-18Co and IMR90 cells were examined by semiquantitative RT-PCR. Right panels, the quantified levels of MSH2, MSH6, MSH3 and MLH1 relative to those of GAPDH. Values are means ±s.d. of three separate experiments.

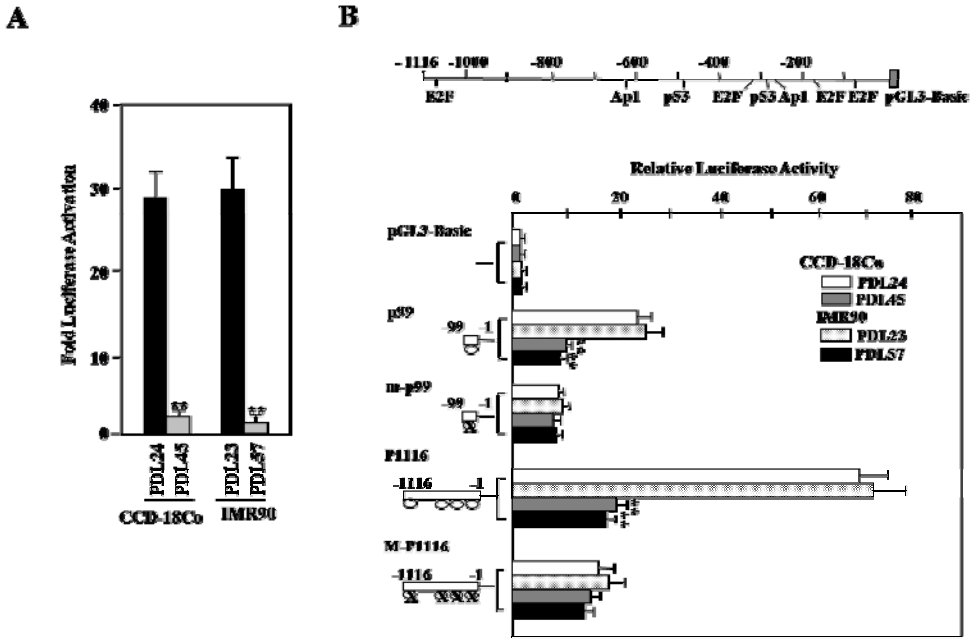
A
B
Fold Luciferase Activation
PDL24
PDL45
PDL23
PDL57
CCD-18Co
IMR90
-1116
-1000
-800
-600
-400
-200
E2F
Ap1
p53
E2F
p53
Ap1
E2F
E2F
pGL3-Basic
Relative Luciferase Activity
pGL3-Basic
p99
m-p99
P1116
M-P1116
CCD-18Co
PDL24
PDL45
IMR90
PDL23
PDL57

Figure 5 Senescence-dependent decreases in MSH2 promoter activity. (A) Young and senescent CCD-18Co and IMR90 cells were co-transfected with the E2F-luc reporter construct containing six E2F responsive sites and the internal control plasmid pRL-CMV, expressing *Renilla* luciferase under the control of the CMV promoter. Relative firefly luciferase activity was calculated by dividing the firefly reading by the *Renilla* luciferase value. Values are represented as the means ±s.d. of three separate experiments. ** denotes P<0.01. (B) Upper panel, the human MSH2 promoter region of the promoter-reporter construct, p1116, showing putative binding sites for E2F, Ap1 and p53. Lower panel, young and senescent CCD-18Co and IMR90 cells were transfected with the indicated plasmids. pGL3-Basic, promoterless luciferase vector; p99, promoter-reporter construct containing position -1 to -99 of the MSH2 promoter; m-p99, p99 containing one mutated E2F-binding motif; p1116, promoter-reporter construct containing position -1 to -p1116 of the MSH2 promoter; m-p1116, p1116 containing four mutated E2F-binding motif. Diagram representations of the promoters are shown; the ovals represent the consensus sites for the E2F binding motifs. Values are represented as the means ±s.d. of three separate experiments. ** denotes P<0.01.

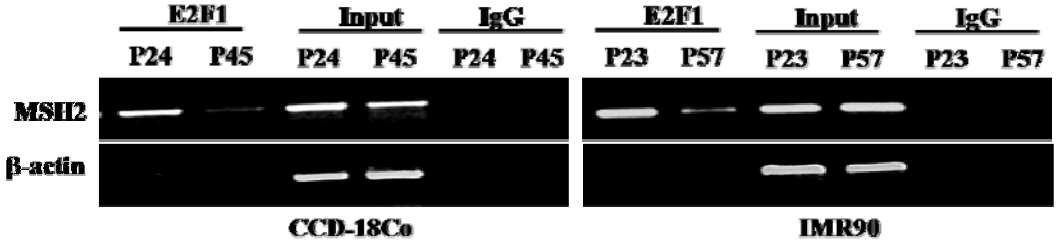
E2F1
Input
IgG
E2F1
Input
IgG
P24
P45
P24
P45
P24
P45
P23
P57
P23
P57
P23
P57
MSH2
β-actin
CCD-18Co
IMR90

Figure 6 Chromatin immunoprecipitation analysis of E2F1 binding to the MSH2 promoter in young and senescent CCD-18Co and IMR90 cells. Chromatin immunoprecipitation assays were performed using E2F1 antibody and anti-mouse IgG (nonspecific) on extracts from young and senescent cells. DNA fragments were amplified by PCR from the promoter regions MSH2 and β-actin. The input chromatin from the young and senescent cells was also amplified by PCR (INPUT) in order to compare the relative amounts of chromatin used in the immunoprecipitation. The data shown are representative of three similar experiments.

Silencing of the E2F1 in young CCD-18Co and IMR90 cells via siRNA lead to a decrease in the MSH2 expression

In order to confirm that E2F1 is indeed essential for MSH2 expression, small interfering RNAs (siRNAs) in the form of two independent, non-overlapping, 21-base pair RNA duplexes, that targeted E2F1 were used in an attempt to inhibit its expression. Young cells were transfected with mock, control siRNA or E2F1 specific siRNAs. Cells were harvested 48 h after transfection, and their protein expression levels were determined. Western blot analysis revealed that the E2F1-specific siRNA oligonucleotides reduced overall E2F1 protein expression by more than 90 %, compared the mock or control siRNA-transfected cells (Figure 7A). The A:C, G:G and G:T mismatch repair activity following E2F1-siRNA transfection was next examined, and it was found that cells with reduced levels of E2F1 expressed significantly lower levels of MSH2 (Figure 7A) and showed reduced all three mismatch repair activity versus mock- or control siRNA-transfected cells (Figure 7B, C).

A

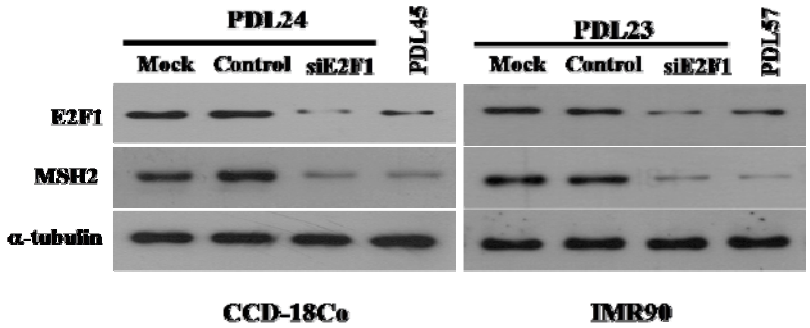
PDL24
Mock
Control
siE2F1
PDL45
PDL23
Mock
Control
siE2F1
PDL57
E2F1
MSH2
α-tubulin
CCD-18Co
IMR90

B

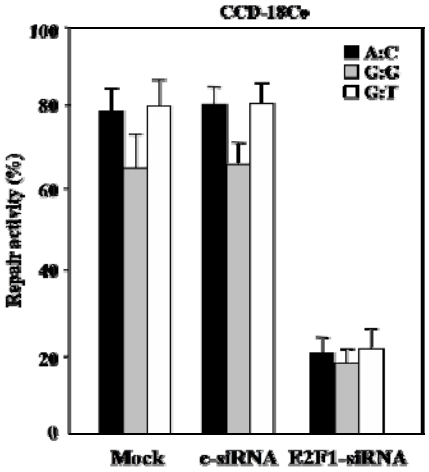
CCD-18Co
A:C
G:G
G:T
Repair activity (%)
0
20
40
60
80
100
Mock
c-siRNA
E2F1-siRNA

C

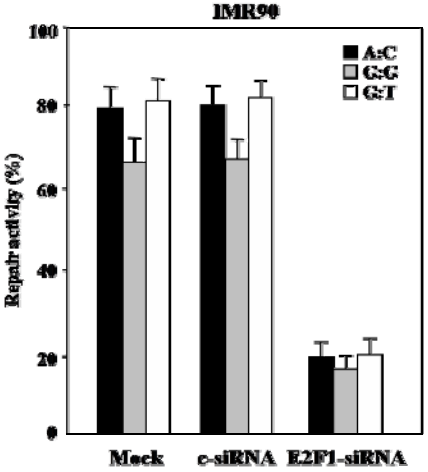
IMR90
A:C
G:G
G:T
Repair activity (%)
0
20
40
60
80
100
Mock
c-siRNA
E2F1-siRNA

Figure 7 siRNA-mediated down-regulation of the E2F1 leads to decrease in MSH2 expression and mismatch repair activity. (A) Mock-, control siRNA-(control), and E2F1-specific siRNA-(siE2F1) transfected young cells, and untreated senescent cells were harvested, and the total lysates were separated on SDS-PAGE and then immunoblotted for E2F1, MSH2 and α-tubulin. (B, C) The nuclear extracts of Mock- and control siRNA-(control), and E2F1-specific siRNA-(siE2F1) transfected young CCD-18Co (B) and IMR90 (C) cells were used to determine the A:C (in black), G:G (in gray) and G:T (in white) mismatch repair efficiencies. The results are based on counting 500-1000 plaques per variable. Values are a mean ±s.d. from three separate experiments.

E2F1-responsive MSH2 is stably repressed in senescent cells but not in quiescent cells

We next analyzed by western blotting from young cells, proliferating in 10 % serum or made quiescent by low-level (0.2 %) serum, and senescent cells. In both quiescent and senescent states, MSH2 expression was suppressed (Figure 8A). However, senescent cells had a greater decrease in MSH2 expression than did quiescent cells. Several E2F1 response genes are known to be stably repressed in senescent cells (35, 36). Thus, MSH2 expression in senescent cells may be resistance to activation by E2F1. To test this hypothesis, we introduced E2F1 into quiescent (serum-starved) or replicative senescent cells using adenovirus-mediated gene transfer and examined the expression of MSH2 expression using semiquantative RT-PCR and western blot 48 hr after infection. Expression of E2F1 in quiescent cells produced a substantial increase in MSH2 mRNA (data not shown) and MSH2 protein (Figure 8B, C). This effect was a result of E2F1 and not adenovirus infection, since a control adenovirus (LacZ) did not induce MSH2. In contrast, E2F1 was unable to effectively induce MSH2 in senescent cells, despite similar levels of E2F1 expression. Therefore, MSH2 is stably repressed in senescent cells.

To confirm whether the stable suppression of the MSH2 could be an important cause of the reduced MMR activity in senescent cells, the adenoviral vector containing E2F1 was infected into the quiescent and senescent cells, and MMR

activities were then measured. We found that the MMR activities was restored in the E2F1 infected quiescent cells, whereas the E2F1 infected senescent cells exhibited no restoration of the MMR activity (Figure 8D).

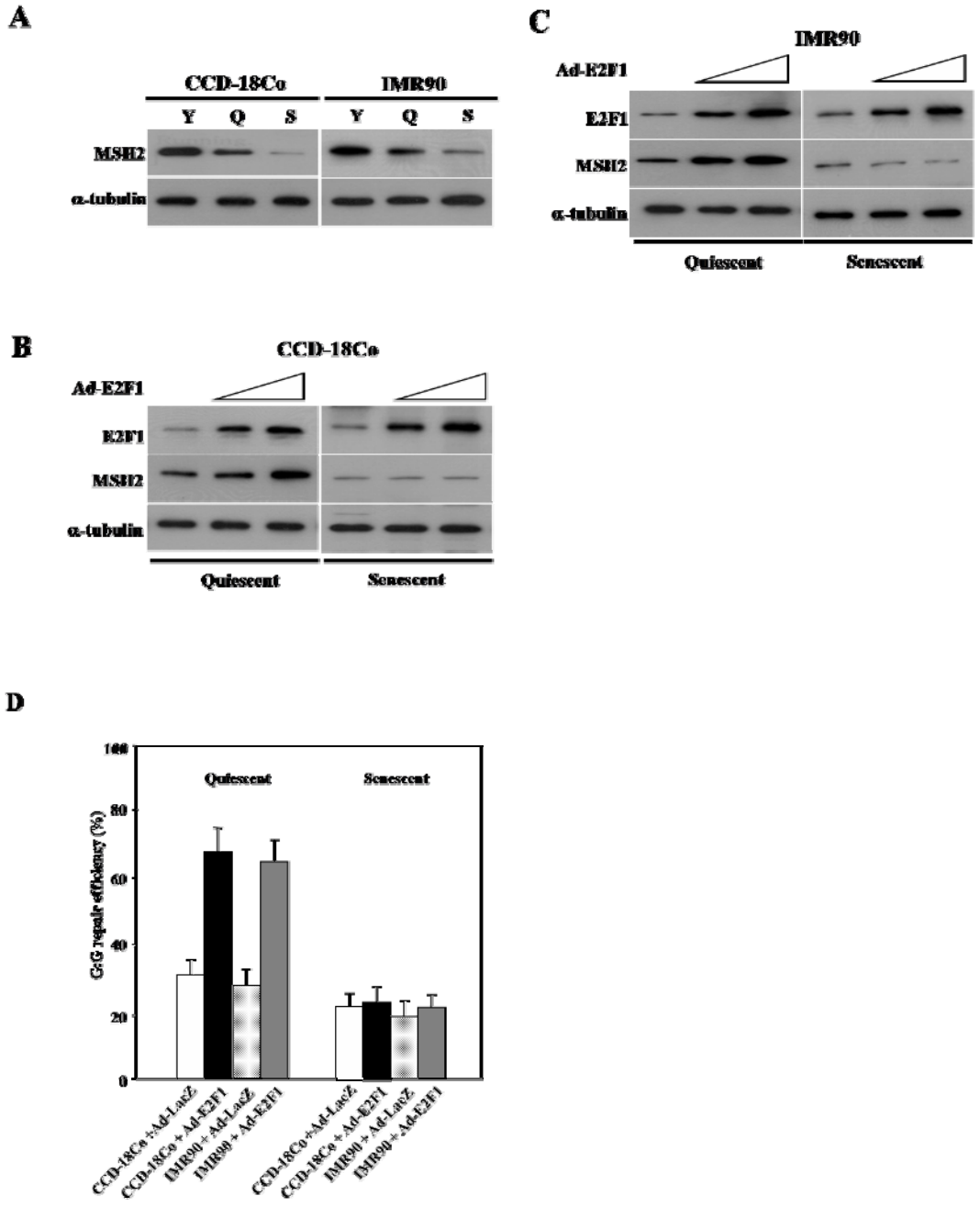
A
CCD-18Co
IMR90
Y
Q
S
Y
Q
S
MSH2
α-tubulin
C
IMR90
Ad-E2F1
E2F1
MSH2
α-tubulin
Quiescent
Senescent
B
CCD-18Co
Ad-E2F1
E2F1
MSH2
α-tubulin
Quiescent
Senescent
D
Quiescent
Senescent
G:G repair efficiency (%)
0
20
40
60
80
100
CCD-18Co+Ad-LacZ
CCD-18Co+Ad-E2F1
IMR90+Ad-LacZ
IMR90+Ad-E2F1
CCD-18Co+Ad-LacZ
CCD-18Co+Ad-E2F1
IMR90+Ad-LacZ
IMR90+Ad-E2F1

Figure 8 MSH2 expression in senescent cells is resistance to activation by E2F1. (A) MSH2 is downregulated in senescent and quiescent cells. Protein extracts of young (Y), quiescent (Q) and senescent (S) CCD-18Co and IMR90 cells were examined by Western blotting using anti-MSH2 antibody. α-tubulin was used as a loading control. (B, C) Quiescent and senescent CCD-18Co (B) and IMR90 (C) cells were infected with adenoviruses expressing LacZ and E2F1. Forty-eight hours after infection, MSH2 level was determined by Western blotting (triangle indicates increasing multiplicities of infections). (D) Quiescent and senescent cells were infected with adenoviruses expressing LacZ and E2F1. Forty-eight hours after infection, the nuclear extracts were used to determine the G:G mismatch repair efficiencies. The results are based on counting 500-1000 plaques per variable. The repair efficiency was calculated as the percentage of decrease in the mixed color colonies. The values are a mean ±s.d. from three separate experiments.

III. DISCUSSION

Considerable evidence implicates an age-dependent accumulation of DNA mutations. For example, an increase in chromosomal aberrations has been observed in aging mice (37, 38). Additionally, aneuploidy translocations and end-to-end fusions have been shown to be higher in peripheral blood lymphocytes and fibroblasts of the elderly than in younger individuals (39-41). Furthermore, splenic and hepatic DNA from different transgenic mice showed increased spontaneous mutation with age (42), and a highly elevated mutation frequency was also observed in the lymphocytes of senescence-accelerated mice (43). More recently, old transgenic Big-Blue™ and Mutra™ mice were shown to contain elevated mutation frequencies (44, 45). In humans, age-related increases in mutation frequency have been found in the *hprt* gene of peripheral blood lymphocytes and kidney epithelial cells (46, 47). Accordingly, it is clear that the process of normal ageing *per se* is associated with an overall deterioration in genome integrity, which might reflect of age-related decline in repair efficiency.

The MMR system is particularly important to the maintenance of genomic integrity. Loss of MMR function results in microsatellite instability and underlies hereditary nonpolyposis colon cancer (48). The primary function of MMR system is to eliminate base-base mismatches and insertion-deletion loops which arise as a consequence of DNA polymerase slippage during DNA replication (12, 48). In

addition to correcting misincorporated nucleotides, MMR proteins have been implicated in double-strand break repair and recombination (13). In particular, MMR recognizes the mismatches in heteroduplex recombination intermediates preventing completion of recombination between diverged sequences, thus promoting genetic stability (49-51). More recently, several groups have shown that MMR is involved in the repair of mismatched 8-oxoguanine, which is one of the major base lesions formed after DNA oxidative attack (52), and may participate in the transcription-coupled repair pathway (53, 54). Cells with a defective MMR demonstrate a mutation rate 100-fold greater than that of normal cells, causing the accumulation of potentially deleterious mutations throughout the genome. These mutations preferentially affect repetitive DNA sequences and are responsible for the occurrence of microsatellite instability (MSI). MSI has been detected in most MMR-deficient tumors and is considered to be the hallmark of hereditary non-polyposis colon cancer (HNPCC) (55-57).

The data presented here show that MMR activity, measured by monitoring the repair of A:C, G:G and G:T mispairs, is markedly reduced in senescent cells as compared with young cells. In order to address the question as to what kind of MMR protein might be involved in the senescence-dependent reduction of MMR activity, we compared the levels of MMR protein in young and senescent cells, and found that MSH2 and MSH6 protein were significantly down-regulated in senescent cells.

In humans, MSH2 can bind to mismatched DNA either alone or when complexed with MSH6 or MSH3 to form MutSα and MutSβ heterodimers, respectively (31). MutSα complex is able to bind to and participate in the repair of single base-base mismatches and of those containing insertion/deletion loops, whereas the MutSβ complex recognizes insertion/deletion loops, which are essentially larger than single base mispairs. Therefore, we next investigated if a reduced MutSα level contributes to the senescence-dependent decline in MMR activity. We purified MutSα and performed MMR assays after adding MutSα to senescent cell extracts, and found that purified MutSα was able to restore MMR activity in the senescent cells. These results suggest that the dysfunction of MutSα contributes to the suppression of MMR activity in senescent cells.

Inactivation of the mouse MSH2 gene was found to result in increase microsatellite instability, a lymphoproliferative disorder, and a predisposition to malignancy (58). In addition, germ-line mutations of hMLH1 and MSH2 are the most frequently impaired genes in HNPCC (59, 60). Moreover, MSH6 mutations are found at high incidence in atypical HNPCC cases that are characterized by cancer onset at age 60 and older (16), and are found in a significant proportion of endometrial cancers (61). Thus, failed recognition and repair of mismatch lesions leads directly to an increase in mutation frequency and malignancy.

Recently, two groups have suggested that MSH2 is an E2F-responsive gene, based on DNA microarray analysis (33, 34). We previously have shown that MSH2

promoter contains several putative E2F binding sites, and the transcriptional activity of E2F1 is important for the expression of MSH2 in human fibroblast GM00637 cells (24). Cellular senescence is an *in vitro* phenomenon involving specific phenotypic changes and proliferative inhibition, and occurs in nontransformed cells following a finite number of cell divisions (62). Proliferation control is primarily achieved in the G1-phase of the cell cycle, the point at which senescent cells arrest. The retinoblastoma protein (pRB) is an important regulator of E2F-responsive gene and contributes to cellular senescence (63). pRB can exist in hyper- and hypophosphorylated forms, the latter binding to and inhibiting a class of transcription factors E2F, the activities of which are required for the transcription genes that are essential for DNA synthesis (64). Phosphorylation of pRB by cyclin-dependent kinases (CDK) leads to the dissociation of the pRB/E2F complex, thus releasing the transcriptional activity of E2F. The activation of E2F is sufficient to commit cells to undergo DNA replication, thus E2F is crucial in the control of cellular proliferation (65). Replicative senescence has been described as irreversible growth arrest occurring after many culture passages, with the overexpression of CDK inhibitors, including $p16^{ink4a}$ (p16) and $p21^{cip/waf1}$ (p21), leading to pRb hypophosphorylation (63, 66). This hypophosphorylation of pRb in senescent cells binds and inhibits E2F, resulting in the suppression of E2F-response genes (67, 68). We have shown that the E2F1 interacts with the putative E2F binding sites of MSH2 promoter, and that this interaction is markedly suppressed in senescent cells. Moreover, it was found that the E2F1-targeted siRNA

oligonucleotides suppressed MSH2 expression and an inhibited MMR activity in young cells. In combination, these findings strongly suggest that the suppression of E2F1 activity contribute, at least in part, to the decrease of expression and/or functional activity of MSH2 in senescent cells.

Much of what we know concerning the regulation of E2F activity comes from studies examining cell cycle transitions into and out of a quiescent state. These transitions are controlled in a reversible manner. In contrast to quiescent cells, mitogenic growth factors are unable to activate E2F target genes in senescent cells (68). Moreover, heterochromatin-associated proteins and the pRB accumulate on the E2F-responsive promoters in senescent but not quiescent cells, and that these changes may be associated with more stable repression of E2F responsive genes (69). Expression of E2F1 in quiescent cells leads to an increase in the E2F-target gene expression, such as MCM3, cyclin A, PCNA, and DHFR. However, E2F1 is unable to effectively induce E2F target genes in senescent cells (35, 69). In the present study, using E2F1 expression viral vectors, we demonstrated that MSH2 is stably repressed in senescent cells but not quiescent cells. Thus, the senescence-dependent suppression of E2F1 activity leads to the stable suppression of MSH2 expression, and hence reduced MMR activity. The epigenetic effects of DNA methylation and their relationship to the transcriptional silencing of growth regulatory genes are important considerations in defining key processes in involved in tumorigenesis (70, 71). Because epigenetic alteration of MMR genes contributes to genomic instability and tumorigenesis (72, 73), epigenetic modification of

MSH2 promoter might be another possible mechanism of MSH2 suppression in senescent cells.

Interestingly, E2F1 knockout mice not only develop normally with a few signs of hypoproliferation but also develop tumors later during their lifetime (36). Although little is known about why the disruption of E2F1 increases rate of carcinogenesis in older adult mice, it is possible that the decline in the MMR activity conveyed by the disruption of E2F1 can explain the increased mutation rate that leads to a higher risk of developing tumors later in life.

To date, conflicting results have been obtained for MMR protein levels at different phases of the cell cycle. For example, several studies have provided evidence indicating that the MMR protein levels are relatively constant throughout the cell cycle (74, 75). However, others have suggested that resting intestinal cells did not express MSH2 (76) and the MMR protein levels exhibited fluctuations (77). Another recent investigation has determined that the expression levels of MMR mRNA and protein are upregulated by growth stimulation (78, 79). In this study, we found that MSH2 expression level and MMR activity were decreased in quiescent cells. This discrepancy of MMR expression levels at discrete phases of the cell cycle may be derived from different cell types, synchronization schemes including serum starvation, mitotic shake-off, and various chemical techniques. Thus, this issue still needs to be studies further to assess the changes of MMR protein level and MMR activity during the cell cycle.

In summary, we show that MMR activity is markedly suppressed in senescent human fibroblast cells, and that this suppression corresponds to demonstrated declines in levels of MSH2 and MSH6 protein (MutSα complex), a known key component in the MMR pathway. Moreover, our results demonstrate that the suppression of E2F1 transcriptional activity in senescent cells is due to down-regulated MSH2 expression, followed by a stimulation of MSH6 degradation, which results in a reduced cellular MMR capacity. Importantly, the expression of E2F1 in quiescent cells resulted in the restoration of E2F1 bound to MSH2 promoter, MSH2 expression and MMR activity, whereas senescent cells expressing E2F1 exhibited no restoration of E2F1 bound to MSH2 promoter, MSH2 expression and MMR activity. Because the suppression of MMR activity directly leads to an increase in the mutation frequency, and finally to malignancy, MMR is believed to play a “caretaker” role by preventing the accumulation of deleterious mutations (13). Therefore, our findings suggest that the suppression of the MMR activity due to MutSα dysfunction may be, at least in part, contributed in the senescence-associated mutagenesis and oncogenesis.

IV. REFERENCES

1. Turker MS. Somatic cell mutations: can they provide a link between aging and cancer? Mech Ageing Dev 2000;117(1-3):1-19.
2. Vijg J. Somatic mutations and aging: a re-evaluation. Mutat Res 2000;447(1):117-35.
3. Moriwaki S, Ray S, Tarone RE, Kraemer KH, Grossman L. The effect of donor age on the processing of UV-damaged DNA by cultured human cells: reduced DNA repair capacity and increased DNA mutability. Mutat Res 1996;364(2):117-23.
4. Goukassian D, Gad F, Yaar M, Eller MS, Nehal US, Gilchrest BA. Mechanisms and implications of the age-associated decrease in DNA repair capacity. Faseb J 2000;14(10):1325-34.
5. Cabelof DC, Raffoul JJ, Yanamadala S, Ganir C, Guo Z, Heydari AR. Attenuation of DNA polymerase beta-dependent base excision repair and increased DMS-induced mutagenicity in aged mice. Mutat Res 2002;500(1-2):135-45.
6. Intano GW, McMahan CA, McCarrey JR, *et al.* Base excision repair is limited by different proteins in male germ cell nuclear extracts prepared from young and old mice. Mol Cell Biol 2002;22(7):2410-8.
7. Chen D, Cao G, Hastings T, *et al.* Age-dependent decline of DNA repair activity for oxidative lesions in rat brain mitochondria. J Neurochem

2002;81(6):1273-84.

8. Szczesny B, Hazra TK, Papaconstantinou J, Mitra S, Boldogh I. Age-dependent deficiency in import of mitochondrial DNA glycosylases required for repair of oxidatively damaged bases. Proc Natl Acad Sci U S A 2003;100(19):10670-5.
9. DePinho RA. The age of cancer. Nature 2000;408(6809):248-54.
10. Campisi J. Cancer and ageing: rival demons? Nat Rev Cancer 2003;3(5):339-49.
11. Mitchell JR, Hoeijmakers JH, Niedernhofer LJ. Divide and conquer: nucleotide excision repair battles cancer and ageing. Curr Opin Cell Biol 2003;15(2):232-40.
12. Kolodner RD, Marsischky GT. Eukaryotic DNA mismatch repair. Curr Opin Genet Dev 1999;9(1):89-96.
13. Harfe BD, Jinks-Robertson S. DNA mismatch repair and genetic instability. Annu Rev Genet 2000;34:359-99.
14. Borresen AL, Lothe RA, Meling GI*, et al.* Somatic mutations in the hMSH2 gene in microsatellite unstable colorectal carcinomas. Hum Mol Genet 1995;4(11):2065-72.
15. Malkhosyan S, Rampino N, Yamamoto H, Perucho M. Frameshift mutator mutations. Nature 1996;382(6591):499-500.
16. Kolodner RD, Tytell JD, Schmeits JL*, et al.* Germ-line msh6 mutations in colorectal cancer families. Cancer Res 1999;59(20):5068-74.

17. Dutkowski RT, Lesh R, Staiano-Coico L, Thaler H, Darlington GJ, Weksler ME. Increased chromosomal instability in lymphocytes from elderly humans. Mutat Res 1985;149(3):505-12.
18. Ganguly BB. Cell division, chromosomal damage and micronucleus formation in peripheral lymphocytes of healthy donors: related to donor's age. Mutat Res 1993;295(3):135-48.
19. Tucker JD, Lee DA, Ramsey MJ, Briner J, Olsen L, Moore DH, 2nd. On the frequency of chromosome exchanges in a control population measured by chromosome painting. Mutat Res 1994;313(2-3):193-202.
20. King CM, Gillespie ES, McKenna PG, Barnett YA. An investigation of mutation as a function of age in humans. Mutat Res 1994;316(2):79-90.
21. Takeda T, Hosokawa M, Higuchi K. Senescence-accelerated mouse (SAM): a novel murine model of senescence. Exp Gerontol 1997;32(1-2):105-9.
22. Nisitani S, Hosokawa M, Sasaki MS, *et al.* Acceleration of chromosome aberrations in senescence-accelerated strains of mice. Mutat Res 1990;237(5-6):221-8.
23. Hosokawa M, Fujisawa H, Ax S, Zahn-Daimler G, Zahn RK. Age-associated DNA damage is accelerated in the senescence-accelerated mice. Mech Ageing Dev 2000;118(1-2):61-70.
24. Youn CK, Cho HJ, Kim SH, *et al.* Bcl-2 expression suppresses mismatch repair activity through inhibition of E2F transcriptional activity. Nat Cell Biol 2005;7(2):137-47.

25. Dimri GP, Lee X, Basile G, *et al.* A biomarker that identifies senescent human cells in culture and in aging skin in vivo. Proc Natl Acad Sci U S A 1995;92(20):9363-7.
26. Drummond JT, Li GM, Longley MJ, Modrich P. Isolation of an hMSH2-p160 heterodimer that restores DNA mismatch repair to tumor cells. Science 1995;268(5219):1909-12.
27. Lee MR, Kim SH, Cho HJ, *et al.* Transcription factors NF-YA regulate the induction of human OGG1 following DNA-alkylating agent methylmethane sulfonate (MMS) treatment. J Biol Chem 2004;279(11):9857-66.
28. Thomas DC, Roberts JD, Kunkel TA. Heteroduplex repair in extracts of human HeLa cells. J Biol Chem 1991;266(6):3744-51.
29. Takeda T, Hosokawa M, Higuchi K. Senescence-accelerated mouse (SAM): a novel murine model of accelerated senescence. J Am Geriatr Soc 1991;39(9):911-9.
30. Takeda T. Senescence-accelerated mouse (SAM): a biogerontological resource in aging research. Neurobiol Aging 1999;20(2):105-10.
31. Fishel R. Mismatch repair, molecular switches, and signal transduction. Genes Dev 1998;12(14):2096-101.
32. Chang DK, Ricciardiello L, Goel A, Chang CL, Boland CR. Steady-state regulation of the human DNA mismatch repair system. J Biol Chem 2000;275(24):18424-31.
33. Polager S, Kalma Y, Berkovich E, Ginsberg D. E2Fs up-regulate expression of

genes involved in DNA replication, DNA repair and mitosis. Oncogene 2002;21(3):437-46.

34. Ren B, Cam H, Takahashi Y, *et al.* E2F integrates cell cycle progression with DNA repair, replication, and G(2)/M checkpoints. Genes Dev 2002;16(2):245-56.
35. Leone G, DeGregori J, Yan Z, *et al.* E2F3 activity is regulated during the cell cycle and is required for the induction of S phase. Genes Dev 1998;12(14):2120-30.
36. Yamasaki L, Jacks T, Bronson R, Goillot E, Harlow E, Dyson NJ. Tumor induction and tissue atrophy in mice lacking E2F-1. Cell 1996;85(4):537-48.
37. Stevenson KG, Curtis HJ. Chromosomal aberrations in irradiated and nitrogen mustard-treated mice. Radiat Res 1961;15:774-84.
38. Tucker JD, Spruill MD, Ramsey MJ, Director AD, Nath J. Frequency of spontaneous chromosome aberrations in mice: effects of age. Mutat Res 1999;425(1):135-41.
39. Ly DH, Lockhart DJ, Lerner RA, Schultz PG. Mitotic misregulation and human aging. Science 2000;287(5462):2486-92.
40. Ramsey MJ, Moore DH, 2nd, Briner JF, *et al.* The effects of age and lifestyle factors on the accumulation of cytogenetic damage as measured by chromosome painting. Mutat Res 1995;338(1-6):95-106.
41. Jacobs PA, Brunton M, Court Brown WM, Doll R, Goldstein H. Change of human chromosome count distribution with age: evidence for a sex differences.

Nature 1963;197:1080-1.

42. Lee AT, DeSimone C, Cerami A, Bucala R. Comparative analysis of DNA mutations in lacI transgenic mice with age. Faseb J 1994;8(8):545-50.
43. Odagiri Y, Uchida H, Hosokawa M, Takemoto K, Morley AA, Takeda T. Accelerated accumulation of somatic mutations in the senescence-accelerated mouse. Nat Genet 1998;19(2):116-7.
44. Walter CA, Grabowski DT, Street KA, Conrad CC, Richardson A. Analysis and modulation of DNA repair in aging. Mech Ageing Dev 1997;98(3):203-22.
45. Ono T, Ikehata H, Nakamura S, *et al.* Age-associated increase of spontaneous mutant frequency and molecular nature of mutation in newborn and old lacZ-transgenic mouse. Mutat Res 2000;447(2):165-77.
46. Wei Q, Matanoski GM, Farmer ER, Hedayati MA, Grossman L. DNA repair and aging in basal cell carcinoma: a molecular epidemiology study. Proc Natl Acad Sci U S A 1993;90(4):1614-8.
47. Martin GM, Ogburn CE, Colgin LM, Gown AM, Edland SD, Monnat RJ, Jr. Somatic mutations are frequent and increase with age in human kidney epithelial cells. Hum Mol Genet 1996;5(2):215-21.
48. Jiricny J, Nystrom-Lahti M. Mismatch repair defects in cancer. Curr Opin Genet Dev 2000;10(2):157-61.
49. Sugawara N, Paques F, Colaiacovo M, Haber JE. Role of Saccharomyces cerevisiae Msh2 and Msh3 repair proteins in double-strand break-induced recombination. Proc Natl Acad Sci U S A 1997;94(17):9214-9.

50. Marsischky GT, Lee S, Griffith J, Kolodner RD. 'Saccharomyces cerevisiae MSH2/6 complex interacts with Holliday junctions and facilitates their cleavage by phage resolution enzymes. J Biol Chem 1999;274(11):7200-6.
51. Mohindra A, Hays LE, Phillips EN, Preston BD, Helleday T, Meuth M. Defects in homologous recombination repair in mismatch-repair-deficient tumour cell lines. Hum Mol Genet 2002;11(18):2189-200.
52. Ni TT, Marsischky GT, Kolodner RD. MSH2 and MSH6 are required for removal of adenine misincorporated opposite 8-oxo-guanine in S. cerevisiae. Mol Cell 1999;4(3):439-44.
53. Mellon I, Rajpal DK, Koi M, Boland CR, Champe GN. Transcription-coupled repair deficiency and mutations in human mismatch repair genes. Science 1996;272(5261):557-60.
54. Mellon I, Champe GN. Products of DNA mismatch repair genes mutS and mutL are required for transcription-coupled nucleotide-excision repair of the lactose operon in Escherichia coli. Proc Natl Acad Sci U S A 1996;93(3):1292-7.
55. Fishel R, Kolodner RD. Identification of mismatch repair genes and their role in the development of cancer. Curr Opin Genet Dev 1995;5(3):382-95.
56. Peltomaki P. Deficient DNA mismatch repair: a common etiologic factor for colon cancer. Hum Mol Genet 2001;10(7):735-40.
57. Peltomaki P. Role of DNA mismatch repair defects in the pathogenesis of human cancer. J Clin Oncol 2003;21(6):1174-9.

58. de Wind N, Dekker M, Berns A, Radman M, te Riele H. Inactivation of the mouse Msh2 gene results in mismatch repair deficiency, methylation tolerance, hyperrecombination, and predisposition to cancer. Cell 1995;82(2):321-30.
59. Hemminki A, Peltomaki P, Mecklin JP, *et al.* Loss of the wild type MLH1 gene is a feature of hereditary nonpolyposis colorectal cancer. Nat Genet 1994;8(4):405-10.
60. Fishel R, Lescoe MK, Rao MR, *et al.* The human mutator gene homolog MSH2 and its association with hereditary nonpolyposis colon cancer. Cell 1993;75(5):1027-38.
61. Wijnen J, de Leeuw W, Vasen H, *et al.* Familial endometrial cancer in female carriers of MSH6 germline mutations. Nat Genet 1999;23(2):142-4.
62. Hayflick L. The Limited In Vitro Lifetime Of Human Diploid Cell Strains. Exp Cell Res 1965;37:614-36.
63. Duncan EL, Wadhwa R, Kaul SC. Senescence and immortalization of human cells. Biogerontology 2000;1(2):103-21.
64. Harbour JW, Dean DC. Rb function in cell-cycle regulation and apoptosis. Nat Cell Biol 2000;2(4):E65-E7.
65. Muller H, Helin K. The E2F transcription factors: key regulators of cell proliferation. Biochim Biophys Acta 2000;1470(1):1-12.
66. Stein GH, Beeson M, Gordon L. Failure to phosphorylate the retinoblastoma gene product in senescent human fibroblasts. Science 1990;249(4969):666-9.
67. Dimri GP, Hara E, Campisi J. Regulation of two E2F-related genes in

presenescent and senescent human fibroblasts. J Biol Chem 1994;269(23):16180-6.

68. Good L, Dimri GP, Campisi J, Chen KY. Regulation of dihydrofolate reductase gene expression and E2F components in human diploid fibroblasts during growth and senescence. J Cell Physiol 1996;168(3):580-8.
69. Narita M, Nunez S, Heard E, *et al.* Rb-mediated heterochromatin formation and silencing of E2F target genes during cellular senescence. Cell 2003;113(6):703-16.
70. Kinzler KW, Vogelstein B. Lessons from hereditary colorectal cancer. Cell 1996;87(2):159-70.
71. Baylin SB, Herman JG. DNA hypermethylation in tumorigenesis: epigenetics joins genetics. Trends Genet 2000;16(4):168-74.
72. Herman JG, Umar A, Polyak K, *et al.* Incidence and functional consequences of hMLH1 promoter hypermethylation in colorectal carcinoma. Proc Natl Acad Sci U S A 1998;95(12):6870-5.
73. Murata H, Khattar NH, Kang Y, Gu L, Li GM. Genetic and epigenetic modification of mismatch repair genes hMSH2 and hMLH1 in sporadic breast cancer with microsatellite instability. Oncogene 2002;21(37):5696-703.
74. Meyers M, Theodosiou M, Acharya S, *et al.* Cell cycle regulation of the human DNA mismatch repair genes hMSH2, hMLH1, and hPMS2. Cancer Res 1997;57(2):206-8.
75. Davis TW, Wilson-Van Patten C, Meyers M, *et al.* Defective expression of the

DNA mismatch repair protein, MLH1, alters G2-M cell cycle checkpoint arrest following ionizing radiation. Cancer Res 1998;58(4):767-78.

76. Leach FS, Polyak K, Burrell M, *et al.* Expression of the human mismatch repair gene hMSH2 in normal and neoplastic tissues. Cancer Res 1996;56(2):235-40.
77. Marra G, Chang CL, Laghi LA, Chauhan DP, Young D, Boland CR. Expression of human MutS homolog 2 (hMSH2) protein in resting and proliferating cells. Oncogene 1996;13(10):2189-96.
78. Iwanaga R, Komori H, Ohtani K. Differential regulation of expression of the mammalian DNA repair genes by growth stimulation. Oncogene 2004;23(53):8581-90.
79. Schroering AG, Edelbrock MA, Richards TJ, Williams KJ. The cell cycle and DNA mismatch repair. Exp Cell Res 2007;313(2):292-304.

<국문초록>

노화과정에서 발생하는 mismatch 복구기능 저하기전

조 향 훈

(지도교수 : 유 호 진)

조선대학교 대학원

의학과

유전자 손상은 노화가 진행되면서 현저하게 증가하지만 아직까지 그 기전에 대해서는 알려진봐 없다. 본 연구에서는 노화에의하여 증가된 유전자 손상의 기전을 규명하고자 mismatch 복구 활성이 젊은세포와 노화세포에서 변하는지 분석하였다. 그 결과 노화세포에서는 젊은세포에 비하여 mismatch 복구 활성이 현저하게 감소됨이 발견되였다. 워스턴 블롯과 면역조직화학 방법으로 mismatch 복구 단백질들을 조사 한결과 노화세포에서 MSH2 및 MSH6 단백질이 현저하게 감소되었다. 전사수준에서의 조절을 검사하기 위하여 두 단백질의 mRNA를 조사한 결과 MSH2의 mRNA가 노화세포에서 감소 되었다. 노화세포에서 감소된 MSH2의 조절 기전을 밝히고자 전사인자를 조사 한 결과 노화세포에서 감소된 E2F1 의 전사 활성이 MSH2의 전사수준에서의 발현을 감소 시킨다는 사실을 규명하였다. 이상의 연구 결과 노화 세포에서는 E2F1의 전사활성이 감소되어 MSH2의 발현이 감소되고 감소된 MSH2는 mismatch 복구활성을 감소시켜 유전자 손상이 노화세포에서 현저하게 증가됨을 알 수 있었다.

저작물 이용 허락서

학 과	의학과	학 번	20047417	과 정	박 사
성 명	한글 : 조 향 훈 한문: 趙 香 勳 영문 : Cho Hyang Hoon				
주 소	광주광역시 북구 일곡동 금호타운 105-501				
연락처	E-MAIL : honch@hahfoc.com				
논문제목	한글 : 노화과정에서 발생하는 mismatch 복구기능 저하 기전 영문 : Molecular mechanisms of senescence-dependent mismatch repair dysfunction				

본인이 저작한 위의 저작물에 대하여 다음과 같은 조건아래 조선대학교가 저작물을 이용할 수 있도록 허락하고 동의합니다.

- 다 음 -

1. 저작물의 DB구축 및 인터넷을 포함한 정보통신망에의 공개를 위한 저작물의 복제, 기억장치에의 저장, 전송 등을 허락함
2. 위의 목적을 위하여 필요한 범위 내에서의 편집·형식상의 변경을 허락함. 다만, 저작물의 내용변경은 금지함.
3. 배포·전송된 저작물의 영리적 목적을 위한 복제, 저장, 전송 등은 금지함.
4. 저작물에 대한 이용기간은 5년으로 하고, 기간종료 3개월 이내에 별도의 의사표시가 없을 경우에는 저작물의 이용기간을 계속 연장함.
5. 해당 저작물의 저작권을 타인에게 양도하거나 또는 출판을 허락을 하였을 경우에는 1개월 이내에 대학에 이를 통보함.
6. 조선대학교는 저작물의 이용허락 이후 해당 저작물로 인하여 발생하는 타인에 의한 권리 침해에 대하여 일체의 법적 책임을 지지 않음
7. 소속대학의 협정기관에 저작물의 제공 및 인터넷 등 정보통신망을 이용한 저작물의 전송·출력을 허락함.

동의 여부: 동의 (0) 반대 ( )

2008 년 2 월 일

저작자: 조 향 훈 (서명 또는 인)

조선대학교 총장 귀하